

---

This is an electronic reprint of the original article.  
This reprint may differ from the original in pagination and typographic detail.

Author(s): Rasilo, Paavo & Abdalh, Ahmed Abou-Elyazied & Belahcen, Anouar & Arkkio, Antero & Dupre, Luc

Title: Identification of Synchronous Machine Magnetization Characteristics From Calorimetric Core-Loss and No-Load Curve Measurements

Year: 2015

Version: Post print

**Please cite the original version:**

Rasilo, Paavo & Abdalh, Ahmed Abou-Elyazied & Belahcen, Anouar & Arkkio, Antero & Dupre, Luc. 2015. Identification of Synchronous Machine Magnetization Characteristics From Calorimetric Core-Loss and No-Load Curve Measurements. IEEE Transactions on Magnetics. Volume 51, Issue 3. 4. ISSN 0018-9464 (printed). DOI: 10.1109/tmag.2014.2354055.

Rights: © 2015 Institute of Electrical & Electronics Engineers (IEEE). Personal use of this material is permitted. Permission from IEEE must be obtained for all other uses, in any current or future media, including reprinting/republishing this material for advertising or promotional purposes, creating new collective works, for resale or redistribution to servers or lists, or reuse of any copyrighted component of this work in other work.

---

All material supplied via Aaltodoc is protected by copyright and other intellectual property rights, and duplication or sale of all or part of any of the repository collections is not permitted, except that material may be duplicated by you for your research use or educational purposes in electronic or print form. You must obtain permission for any other use. Electronic or print copies may not be offered, whether for sale or otherwise to anyone who is not an authorised user.

© 2014 IEEE. Personal use of this material is permitted. Permission from IEEE must be obtained for all other uses, in any current or future media, including reprinting/republishing this material for advertising or promotional purposes, creating new collective works, for resale or redistribution to servers or lists, or reuse of any copyrighted component of this work in other works.

# Identification of Synchronous Machine Magnetization Characteristics from Calorimetric Core-Loss and No-Load Curve Measurements

P. Rasilo<sup>1</sup>, A. Abdalh<sup>2,3</sup>, A. Belahcen<sup>1</sup>, A. Arkkio<sup>1</sup>, and L. Dupré<sup>2</sup>

<sup>1</sup>Department of Electrical Engineering and Automation, Aalto University School of Electrical Engineering, P.O. Box. 13000, FI-00076 Espoo, Finland

<sup>2</sup>Department of Electrical Energy, Systems and Automation, Ghent University, Sint-Pietersnieuwstraat 41, BE-9000 Ghent, Belgium

<sup>3</sup>Electrical Power & Machines Department, Cairo University, EG-12613 Giza, Egypt

The magnetic material characteristics of a wound-field synchronous machine are identified based on global calorimetric core-loss and no-load curve measurements. This is accomplished by solving a coupled experimental-numerical electromagnetic inverse problem, formulated to minimize the difference between a finite-element (FE) simulation-based Kriging surrogate model and the measurement results. The core-loss estimation in the FE model is based on combining a dynamic iron-loss model and a static vector Jiles-Atherton hysteresis model, the parameters for which are obtained by solving the inverse problem. The results show that reasonable hysteresis loops can be produced for a grid-supplied machine, while for an inverter-supplied machine the limitations in the FE and iron-loss models seemingly exaggerate the area of the loop. In addition, the effect of the measurement uncertainty on the inverse problem is quantitatively estimated.

**Index Terms**—Calorimetric loss measurements, electromagnetic inverse problems, iron losses, magnetic hysteresis, synchronous machines.

## I. INTRODUCTION

THE magnetic characteristics of the core laminations of electrical machines are typically deteriorated as a result of the manufacturing process [1], especially punching [2]. Since simulation models are typically identified with measurements from separate lamination samples, modeling results may differ significantly from measurements done for a processed and assembled machine. Especially, the core losses are often underestimated, since the loss properties of the processed laminations are not known accurately.

A wide range of different modeling techniques have been proposed to improve the loss calculation for the processed cores. Both [3] and [4] approached the problem in a *forward* manner, meaning that the experimentally or analytically determined degraded material properties were input to finite-element (FE) models as parameters, and the core losses were obtained as the outputs from the models. On the contrary, a *stochastic* approach was presented in [5], in which probabilistic models were developed for the magnetization curves and iron-loss coefficients of a stator core material by utilizing experimental data from 28 stators.

The third possibility is to approach the problem in an *inverse* manner with the aim of obtaining deterministic material properties starting from well-defined global and/or local measurements. Such approaches typically iteratively search for the optimal values of the magnetic material parameters, which minimize the difference between simulation and measurement results [6], [7]. For example, in [8], the magnetization properties of an EI-core inductor were determined by comparing

measurements to simulation results from an FE tool coupled to an analytical Preisach hysteresis model. In [9], the loss parameters of an asynchronous motor core were recovered using a similar methodology. A good correspondence was observed to results from standard ring-core measurements.

In this paper, we adopt a new formulation of the experimental-numerical inverse approach for determining the magnetic material characteristics of a 150-kVA wound-field synchronous machine, whose core losses have been determined experimentally using calorimetric measurements. However, our loss models identified from the standard Epstein-frame measurements of the original steel strips underestimate these core losses [10]. Here we assume that this underestimation is mainly caused by deterioration of the hysteresis characteristics of the machine, and thus attempt to find such effective magnetization characteristics that give a better correspondence between the measurements and the simulations. Since the inverse problem based only on the core-loss measurements is an ill-posed problem, we solve the problem instead for a multi-objective function, including also the no-load curve measurements in addition to the core losses.

The simulations are done with a 2-D time-stepping FE method including models for the hysteresis, eddy-current and excess losses in the core laminations. The magnetization curves are analytically modeled with a vector Jiles-Atherton (J-A) hysteresis model with seven independent parameters. Since the FE model is computationally heavy, and thus impractical for the proposed inverse approach, we first build a fast Kriging surrogate model that accurately emulates the FE model. The inverse identification problem is then formulated to find the seven parameters of the J-A model by iteratively minimizing the difference between the FE-Kriging modeled and measured core losses and no-load curves. The material properties are solved for both grid- and inverter-supplied machines. In addition, the effect of the measurement error on the inverse problem results is demonstrated.

Manuscript received May 15, 2014. Corresponding author: P. Rasilo (email: paavo.rasilo@aalto.fi).

P. Rasilo acknowledges the Finnish Foundation for Technology Promotion for financial support. A. Abdalh gratefully acknowledges the financial support of the Special Research Fund (BOF) of Ghent University. The research leading to these results has received funding from the European Research Council under the European Union's Seventh Framework Programme (FP7/2007-2013) / ERC grant agreement n° 339380.

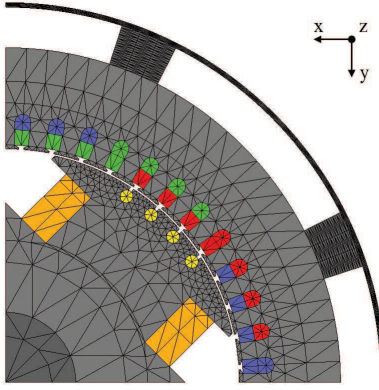


Fig. 1. FE mesh of the test machine including the stator frame. The meshes of the air regions are not shown for clarity.

## II. METHODS

### A. Test Machine and Measurement Setup

The test machine is a 150-kVA 400-V, 50-Hz, 4-pole synchronous generator designed for a diesel-generator application. The cross-sectional geometry and FE mesh are shown in Fig. 1. Both the stator and the rotor cores of the machine are stacked of M600/50A Fe-Si steel sheets, whose magnetic properties have been determined by Epstein-frame measurements. The core losses of the machine have been measured using an open-cycle air-cooled calorimetric system [10].

The calorimetric setup has been calibrated with DC heater resistors while rotating the test machine unexcited and thus allows direct determination of the total electromagnetic losses of the machine by the comparison of the heat transferred by the cooling air to the calibration curve. The core losses are obtained by subtracting the stator and rotor DC resistive losses from the total electromagnetic losses. The measurement errors for the core losses are 5.8 – 9.6%, depending on the loading point and the type of supply [10]. The measurement results with grid and PWM inverter supplies at different loads are presented in Table I. The switching frequency in the PWM is 6 kHz.

The terminal quantities of the machine were measured with a LEM Norma D 6000 power analyzer. The no-load curves were measured by recording the stator terminal voltages in open-circuit operation with different rotor currents.

### B. FE Model with Iron Losses

The test machine is modeled with a 2-D FE method using a magnetic vector potential formulation, with  $\mathbf{A} = A\mathbf{u}_z$  and  $\mathbf{B} = \nabla \times \mathbf{A}$  being the magnetic vector potential and the flux density, respectively. The field equations are coupled to the circuit equations of the stator and field windings in order to allow the simulation with a voltage supply. To include the iron losses into the solution, Ampere's law in the iron regions is written as

$$\nabla \times \mathbf{H}_{\text{Fe}} = \mathbf{0} \quad (1)$$

in which  $\mathbf{H}_{\text{Fe}}$  includes the static hysteretic, classical eddy-current and excess parts, respectively:

$$\mathbf{H}_{\text{Fe}} = \mathbf{H}_{\text{st}}(\mathbf{B}) + \frac{\sigma d^2}{12} \frac{\partial \mathbf{B}}{\partial t} + c_{\text{ex}} \left| \frac{\partial \mathbf{B}}{\partial t} \right|^{-0.5} \frac{\partial \mathbf{B}}{\partial t}, \quad (2)$$

TABLE I  
MEASURED CORE LOSSES AND MEASUREMENT ERRORS IN DIFFERENT LOADING POINTS AND WITH DIFFERENT VOLTAGE WAVEFORMS

Load	25%	50%	75%	100%
Grid	1363 W ±102 W (7.5%)	1562 W ±114 W (7.3%)	1742 W ±138 W (7.9%)	2019 W ±194 W (9.6%)
PWM	1836 W ±106 W (5.8%)	1944 W ±117 W (6.0%)	2154 W ±146 W (6.8%)	2397 W ±204 W (8.5%)

with  $\sigma = 3.00 \text{ MS/m}$ , and  $d = 0.5 \text{ mm}$  being the conductivity and thickness of the lamination material, respectively.  $c_{\text{ex}} = 0.718 \text{ W/m}^3 (\text{s/T})^{3/2}$  is the coefficient for the excess losses as described in [10].

The static hysteretic field strength  $\mathbf{H}_{\text{st}}(\mathbf{B})$  is modeled with the vector J-A model comprehensively described in [11]. The only difference to the model of [11] is that the sum of two Langevin functions  $\mathfrak{L}(x) = \coth x - 1/x$  is used to describe the relationship between the anhysteretic magnetization  $\mathbf{M}_{\text{an}}$  and the effective field strength  $\mathbf{H}_{\text{eff}}$  in order to allow greater variation in the shapes of the hysteresis loops:

$$\mathbf{M}_{\text{an}} = \frac{\mathbf{H}_{\text{eff}}}{|\mathbf{H}_{\text{eff}}|} \sum_{i=1}^2 m_i \mathfrak{L} \left( \frac{|\mathbf{H}_{\text{eff}}|}{a_i} \right). \quad (3)$$

The hysteresis loops are thus analytically described by the 7 constant parameters  $a_1$ ,  $a_2$ ,  $m_1$ ,  $m_2$ , and  $\alpha$ ,  $c$  and  $k$  of the traditional J-A model [11].

To ensure a good convergence during the FE solution with a wide range of different  $B$ - $H$  loops, the irreversible curve is neglected during the solution and only the shape of the anhysteretic curve is used, while the hysteresis losses are calculated *a posteriori* with the full J-A model. In [12], it has been shown that the errors caused by this assumption are small and thus justified in order to improve the convergence. Thus, during the FE solution, the field strength as a function of the flux density is iterated from:

$$\nu_0 \mathbf{B} - \mathbf{H}_{\text{st}} = \frac{\mathbf{H}_{\text{st}}}{|\mathbf{H}_{\text{st}}|} \sum_{i=1}^2 m_i \mathfrak{L} \left( \frac{|\mathbf{H}_{\text{st}}|}{a_i} \right). \quad (4)$$

For each loading point, all the time-stepping FE simulations were started from the same initial conditions obtained with a static solver in which the single-valued magnetization characteristics were used. Several supply periods were then simulated in order to reach a steady state. The loading point of the time-stepping FE model thus depends on the J-A parameters. In order to compare the losses in the loading points of Table I, the simulation results were interpolated to the corresponding loads. The no-load curves were calculated with the static FE model with source currents in the rotor and by assuming sinusoidal time-variation of the stator flux linkages.

### C. Inverse Problem Approach

The inverse problem is formulated to find the optimum set of parameters  $\tilde{\mathbf{x}} = (a_1, a_2, m_1, m_2, \alpha, c, k)$  which minimizes the difference between sets of FE-modeled and measured core-loss values  $\mathbf{P}$ . In this case, vectors  $\mathbf{P}$  include the values in the four loading points of Table I.

Since both the simulated loading points and losses depend on the J-A parameters, it is difficult to prove the uniqueness of the inverse problem solution. It seems possible, however, that comparison of the core-loss curves alone does not guarantee a unique solution. Thus, in addition to the loss curves  $\mathbf{P}$ , eight simulated no-load voltage points  $\mathbf{V}_0$  of the machine are compared to measured ones. In open circuit operation, the relationship between the rotor current and the terminal voltage is mainly determined by the magnetization properties, and thus comparison of the no-load curves should ensure that physically reasonable hysteresis loop shapes are obtained. The inverse problem with the multi-objective function  $F$  is thus written as

$$\tilde{\mathbf{x}} = \underset{\mathbf{x}}{\operatorname{argmin}} F(\mathbf{x}) \quad (5)$$

$$F(\mathbf{x}) = \left\| \frac{\mathbf{P}_{\text{sim}}(\mathbf{x}) - \mathbf{P}_{\text{meas}}}{\mathbf{P}_{\text{meas}}} \right\|^2 + \left\| \frac{\mathbf{V}_{0,\text{sim}}(\mathbf{x}) - \mathbf{V}_{0,\text{meas}}}{\mathbf{V}_{0,\text{meas}}} \right\|^2, \quad (6)$$

in which the sum of the norms of the relative differences between the measurements and simulations is minimized.

The time-stepping FE calculation of the 4 loading points takes almost 1.5 hours and is thus impractical for the iterative procedure (5). We thus first built a Kriging surrogate model for fast emulation of the FE model. This surrogate model was based on FE simulations with 100 different parameter sets  $\mathbf{x}$  producing a wide variety of different  $B$ - $H$  loops. The 100 parameter sets were scattered throughout the following design space (relative to the initial parameters of Table II) using the Latin hypercube sampling method:

- $a_1, a_2 \in [0.5, 5.0]$
- $m_1, m_2 \in [0.8, 1.2]$
- $\alpha, c, k \in [0.5, 2.0]$ .

The accuracy of the model was assessed as shown in [13]. The surrogate model allows obtaining  $\mathbf{P}_{\text{sim}}(\mathbf{x})$  and  $\mathbf{V}_{0,\text{sim}}(\mathbf{x})$  in (6) in approximately 5 seconds and is thus suitable for the inverse problem.

### III. RESULTS AND DISCUSSION

#### A. Forward Approach for Loss Estimation

We first estimate the core losses of the machine in the typical forward manner using a  $B$ - $H$  loop directly fitted to the Epstein-strip measurements. Table II shows the J-A model parameters obtained with the fitting, while Fig. 2 shows the fitted loops and compares the resulting FE-calculated core losses and no-load curves to the measurements. It is seen that the core losses are underestimated especially at higher loads, which is at least partly caused by the differences between the  $B$ - $H$  loops of the processed core and those of the Epstein strips. In addition, the no-load curve is slightly underestimated in the high saturation. This is the motivation of solving the inverse problem in order to find a better correspondence to the measurement results.

TABLE II

J-A MODEL PARAMETERS FITTED TO THE EPSTEIN MEASUREMENTS

$a_1$	$a_2$	$m_1$	$m_2$	$\alpha$	$c$	$k$
2130 A/m	27.8 A/m	223 kA/m	1186 kA/m	$1.1 \times 10^{-4}$	0.371	112 A/m

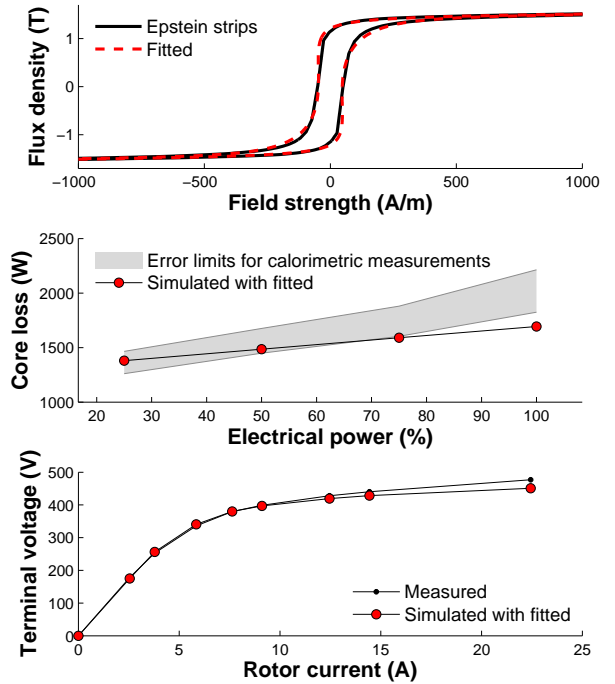


Fig. 2. The  $B$ - $H$  loop measured from Epstein strips, J-A parameters obtained by the least-squares fitting, and comparison of corresponding FE simulation results to the core-loss and no-load curve measurements.

#### B. Results for Grid- and PWM-Supplied Machines

Fig. 3 shows the inverse problem solution for the machine with both grid and PWM supplies. It is seen that the  $B$ - $H$  loop obtained with the grid supply is flatter than the one measured from the Epstein strips. This seems physically reasonable and implies that the material properties of the machine have been deteriorated because of the manufacturing defects, as initially expected. The flatter  $B$ - $H$  curve causes the simulated core losses to be higher than those in Fig. 2, and thus gives a better correspondence to the calorimetric measurements. Also the no-load curve is very well modeled up to high saturation.

In the case of the PWM supply, however, the obtained  $B$ - $H$  loop is wider than the Epstein-measured one. This is caused by the fact that the J-A model does not model correctly the minor hysteresis loops which causes increased hysteresis losses in the actual machine with a PWM supply. In addition, the PWM supply also increases the eddy-current losses in, for example, the stator windings and the end-plates, which are not taken into account in the model. In the inverse problem solution these limitations are compensated by an increased loop area to get a good correspondence to the measured core losses.

#### C. Effect of Measurement Uncertainty

Fig. 4 shows the inverse problem solutions in which the lower (lb) and upper (ub) measurement error bounds of the grid-supplied machine are used as the targets. Both of the recovered  $B$ - $H$  loops have a lower permeability than the Epstein strips, which is explained by the material degradation. Moreover, the measurement uncertainty has a limited effect on the inverse problem solution, since almost similar loops were obtained for the lower and upper error limits.

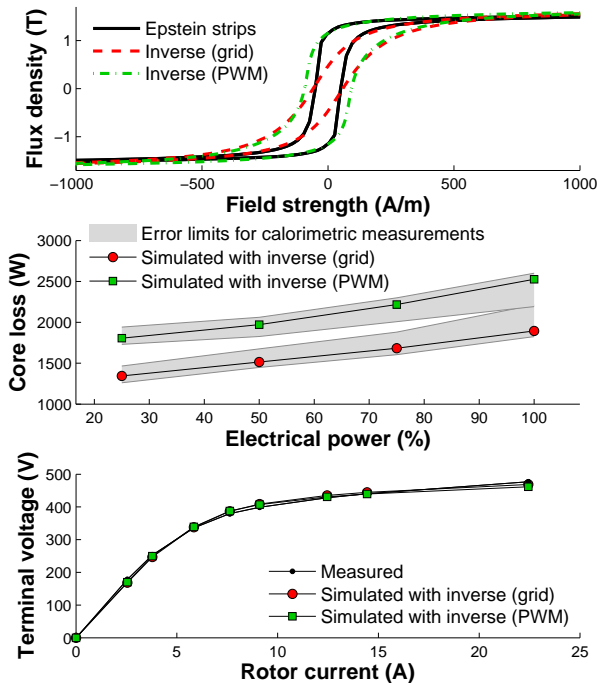


Fig. 3. The reconstructed  $B$ - $H$  loops for grid and PWM supplies, and comparison of corresponding FE simulation results to the core-loss and no-load curve measurements.

#### IV. CONCLUSION

It was shown that reasonable magnetization characteristics for a synchronous machine can be recovered starting from calorimetric core-loss and no-load curve measurements. We emphasize that the Epstein-strip measurements were used merely to obtain suitable parameter variation limits for constructing the surrogate model and to have a reference for the curves solved from the inverse problem. The presented methods are thus applicable even without prior knowledge on the magnetization curves, if the parameter ranges can be defined by some other means (e.g. using the ranges proposed here as a starting point).

Different magnetization properties were retrieved for grid- and inverter-supplied machines. This is caused by the simplifications of the 2-D FE model and the  $J$ - $A$  hysteresis model which lead to underestimation of the PWM losses. The quality of the inverse problem solution is thus limited by the accuracy of the used models. In addition, we showed that the effect of the measurement uncertainty on the accuracy of the inverse problem is small, which proves the effectiveness of the proposed inverse methodology.

Finally, it is worth mentioning that the obtained  $B$ - $H$  loops do not represent the actual material properties but rather effective properties which give a reasonable global behavior for the machine. In practice, the magnetization properties of the core vary locally due to spatially varying stress distributions in the machine.

#### REFERENCES

[1] B. Vaseghi, S. A. Rahman, and A. M. Knight, "Influence of steel manufacturing on  $J$ - $A$  model parameters and magnetic properties," *IEEE Trans. Magn.*, Vol. 49, No. 5, pp. 1961-1964, May 2013.

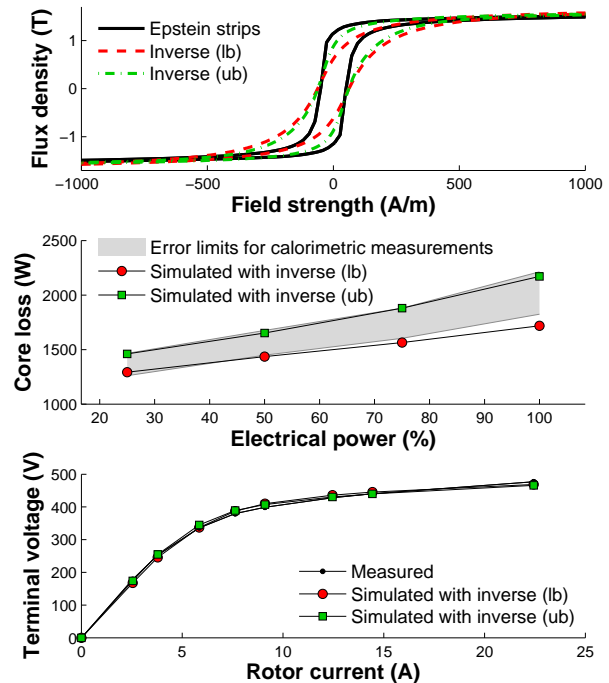


Fig. 4. The reconstructed  $B$ - $H$  loops for the upper and lower error limits with grid supply, and comparison of corresponding FE simulation results to the core-loss and no-load curve measurements.

[2] F. Ossart, E. Hug, O. Hubert, C. Buvat, R. Billardon, "Effect of Punching on Electrical Steels: Experimental and Numerical Coupled Analysis," *IEEE Trans. Magn.*, Vol. 36, No. 5, pp. 3137-3140, September 2000.

[3] K. Fujisaki, R. Hiriyama, T. Kawachi, S. Satou, C. Kaidou, M. Yabumoto, and T. Kubota, "Motor Core Iron Loss Analysis Evaluating Shrink Fitting and Stamping by Finite-Element Method," *IEEE Trans. Magn.*, Vol. 43, No. 5, pp. 1950-1954, May 2007.

[4] M. Bali, H. De Gersem, and A. Muetze, "Finite-Element Modeling of Magnetic Material Degradation Due to Punching," *IEEE Trans. Magn.*, Vol. 50, No. 2, Art. No. 7018404, February 2014.

[5] R. Ramaratofika, A. Benabou, and S. Clénet, "Stochastic Modeling of Soft Magnetic Properties of Electrical Steels: Application to Stators of Electrical Machines," *IEEE Trans. Magn.*, Vol. 48, No. 10, pp. 2573-2584, October 2012.

[6] A. Tarantola, "Inverse problem theory and methods for model parameter estimation," Society for industrial and applied mathematics (SIAM), Philadelphia, USA, 2004.

[7] D. Ioan, M. Rebian, "Extraction of B-H relation based on the inverse magnetostatic problem," *Int. J. Appl. Electrom.*, Vol. 13, pp. 329-334, 2001/2002.

[8] A. A.-E. Abdallah, P. Sergeant, G. Crevecoeur, and L. Dupré, "An Inverse Approach for Magnetic Material Characterization of an EI Core Electromagnetic Inductor," *IEEE Trans. Magn.*, Vol. 46, No. 2, pp. 622-625, February 2010.

[9] A. A.-E. Abdallah, P. Sergeant, and L. Dupré, "A non-destructive methodology for estimating the magnetic material properties of an asynchronous motor," *IEEE Trans. Magn.*, Vol. 48, No. 4, pp. 1621-1627, April 2012.

[10] P. Rasilo, A. Belahcen, and A. Arkkio, "Experimental determination and numerical evaluation of core losses in a 150-kVA wound-field synchronous machine," *IET Electr. Power Appl.*, Vol. 7, No. 2, pp. 97-105, February 2013.

[11] J. Gyselinck, P. Dular, N. Sadowski, J. Leite, and J. P. A. Bastos, "Incorporation of a Jiles-Atherton vector hysteresis model in 2D FE magnetic field computations," *COMPEL*, Vol. 23, No. 3, pp. 685-693, 2004.

[12] P. Rasilo, A. Belahcen, and A. Arkkio, "Importance of Iron-Loss Modeling in Simulation of Wound-Field Synchronous Machines," *IEEE Trans. Magn.*, Vol. 48, No. 9, pp. 2495-2504, September 2012.

[13] L. Wang and D. Lowther, "Selection of approximation models for electromagnetic device optimization," *IEEE Trans. Magn.*, Vol. 42, No. 4, pp. 1227-1230, April 2006.